PHYSICAL REVIEW B **91**, 081114(R) (2015)

Ultrafast charge and lattice dynamics in one-dimensional Mott insulator of CuO-chain compound Ca_2CuO_3 investigated by femtosecond absorption spectroscopy

H. Matsuzaki,[1,*] H. Nishioka,[1] H. Uemura,[1] A. Sawa,[2] S. Sota,[3] T. Tohyama,[4] and H. Okamoto[1]

[1]*Department of Advanced Materials Science, Graduate School of Frontier Sciences, University of Tokyo, 5-1-5 Kashiwanoha, Kashiwa, Chiba 277-8561, Japan*

[2]*National Institute of Advanced Industrial Science and Technology (AIST), Tsukuba Central 4, 1-1-1 Higashi, Tsukuba, Ibaraki 305-8562, Japan*

[3]*Computational Materials Science Research Team, RIKEN Advanced Institute for Computational Science (AICS), Kobe, Hyogo 650-0047, Japan*

[4]*Department of Applied Physics, Tokyo University of Science, Katsushika, Tokyo 125-8585, Japan*

(Received 2 December 2014; revised manuscript received 5 February 2015; published 27 February 2015)

Charge dynamics in one-dimensional (1D) Mott insulators was investigated by femtosecond pump-probe absorption spectroscopy on Ca_2CuO_3. An irradiation of a femtosecond laser pulse gives rise to a Drude-like response due to the nature of spin-charge separation characteristic of 1D Mott insulators. The photoinduced metallic state decays with ∼30 fs, and photocarriers are localized as polarons via charge-phonon coupling which produce a broad midgap absorption. Calculations with the extended Hubbard-Holstein model suggest that the peak structure of the midgap absorption is a magnon sideband of the polaron absorption. This demonstrates that charge-spin coupling becomes effective via charge-phonon coupling in polarons.

DOI: 10.1103/PhysRevB.91.081114 PACS number(s): 71.20.Nr, 71.38.−k, 78.20.−e, 78.47.−p

In various kinds of perovskite-type oxides, Mott insulator to metal transitions are induced by chemical carrier doping [1]. It is expected that similar metallizations of Mott insulators are driven by photoirradiation via creations of electron and hole carriers, that is, by "photocarrier doping." Such attempts have been performed not only in oxides [2–14], but also in other correlated-electron materials [15–24]. In particular, in one-dimensional (1D) Mott insulators of halogen-bridged Ni- and Pd-chain compounds, $[Ni(chxn)_2Br]Br_2$ (chxn = cyclohexanediamine) [19] and $[Pd(en)_2Br](C_5\text{-}Y)_2H_2O$ (en = ethylenediamine, C_5-Y = dialkylsulfosuccinate) [20], and an organic molecular compound, ET-F_2TCNQ [ET = bis(ethylenedithio)tetrathiafulvalene and F_2 TCNQ = difluoro-tetracyanoquinodimethane] [21], photoinduced metallizations were demonstrated by the observations of clear Drude responses in the infrared region. These phenomena are consistent with a theoretical prediction that a carrier doping to a 1D Mott insulator necessarily induces a metallization of the system irrespective of carrier density. Such a metallization originates from the nature of spin-charge separation characteristic of 1D correlated-electron systems [25,26].

More recently, photoinduced metallizations were investigated in two-dimensional (2D) Mott insulators of the cuprates, Nd_2CuO_4 and La_2CuO_4 [10,11]. In these compounds, Drude responses also appeared by photoirradiation; however, their spectral weights were smaller than those of midgap absorptions due to photocarriers localized via the charge-spin coupling inherent to 2D correlated-electron systems. Such features are in contrast to those of 1D Mott insulators, in which photoresponses are dominated by Drude responses. In addition, it was pointed out that the effect of charge-phonon coupling cannot be neglected in the 2D cuprates [10,11,27–32]. In general, charge-phonon coupling is more effective in 1D systems than in 2D ones, so that it is important to clarify the role of charge-phonon coupling in photoresponses of 1D Mott insulators [33], which might compete against a metallization and/or give rise to charge-spin coupling. In the present study, we investigated photoresponses in a 1D Mott insulator of a cuprate, Ca_2CuO_3, by femtosecond pump-probe (PP) absorption spectroscopy. The result reveals that a Drude-like response is photoinduced, but it decays very rapidly and photocarriers are localized by charge-phonon coupling, showing a broad midgap absorption. Theoretical analyses with the extended Holstein-Hubbard model demonstrate that the spectral shape of the midgap absorption is dominated by a magnon sideband of the polaron absorption.

Crystal structure of Ca_2CuO_3 is shown in Fig. 1(a) [34]. A CuO-chain consists of CuO_4 quadrilaterals sharing corner oxygens along the b axis. As shown in the lower part of Fig. 1(a), a Cu ion is divalent ($S = 1/2$) and one unpaired electron exists in the $d_{x^2-y^2}$ orbital. A 1D electronic state is formed by the overlap of p_x and p_y orbitals of O and $d_{x^2-y^2}$ orbitals of Cu. Because of large on-site Coulomb repulsion energy U on Cu ions, a Mott-Hubbard gap is opened in the Cu $3d$ band as shown in Fig. 1(b). An occupied O $2p$ valence band is located between the Cu $3d$ upper Hubbard (UH) band and the lower Hubbard band. Thus, Ca_2CuO_3 is a charge-transfer (CT) insulator, and the lowest optical transition is a CT-gap transition from the O $2p$ valence band to the Cu $3d$ UH band [the open arrow in Fig. 1(b)].

Epitaxial thin films of Ca_2CuO_3 with a thickness of 60 nm were fabricated on anisotropic substrates, $LaSrAlO_4(100)$ by a graphoepitaxial laser-ablation technique [35,36]. The growth method and characterization of the film are detailed in the Supplemental Material S1 [37]. For the PP measurements, we used two systems in which a temporal width of a laser pulse

*Present address: Research Institute of Instrumentation Frontier, National Institute of Advanced Industrial Science and Technology (AIST), Tsukuba Central 2, 1-1-1 Umezono, Tsukuba, Ibaraki 305-8568, Japan.

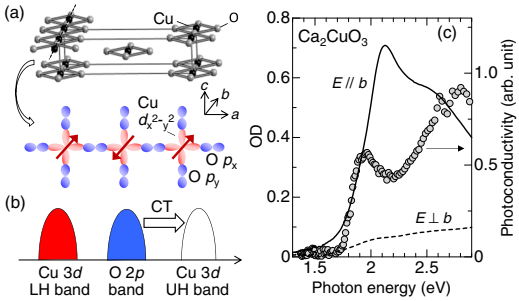

FIG. 1. (Color online) (a) Crystal structures of Ca_2CuO_3. Ca atoms are omitted for simplicity. 1D electronic state is formed by the $d_{x^2-y^2}$ orbital of Cu, and the p_x (p_y) orbital of O. (b) Electronic structure and CT transition of Ca_2CuO_3. (c) Polarized absorption (OD) spectrum with light electric fields (E) ∥ and ⊥ b (chain axis). Circles show the excitation profile of photoconductivity along b in a single crystal of Ca_2CuO_3 [38].

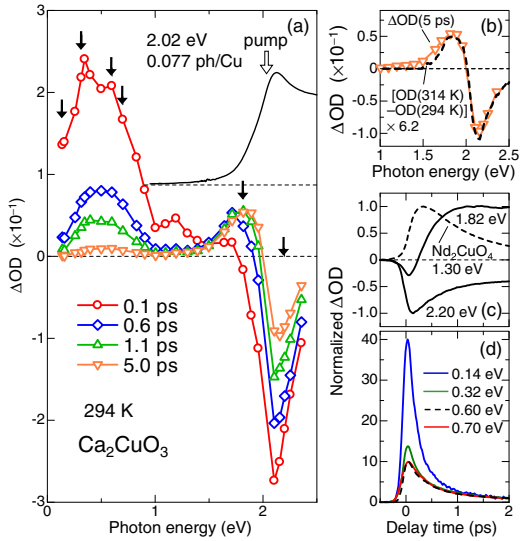

FIG. 2. (Color online) (a) Photoinduced absorption (ΔOD) spectra by the 2.02-eV pump ($x_{ph} = 0.077$ ph/Cu) in Ca_2CuO_3. The time resolution is 200 fs. The solid line shows the OD spectrum along b. (b) The ΔOD spectrum at 5 ps. The broken line shows the differential OD spectrum [OD(314 K)−OD(294 K)]. (c) Time profiles of ΔOD in the CT-gap-transition region normalized by the maximum values of |ΔOD|. The broken line shows the time profile of ΔOD at 1.30 eV in Nd_2CuO_4 measured with the time resolution of 200 fs [10]. (d) Time profiles of ΔOD in the inner-gap region normalized at 2 ps.

(the time resolution) is 130 fs (200 fs) and 24 fs (34 fs). Details of the PP setups are also reported in the Supplemental Material S2 [37]. Delay time t_d of the probe pulse relative to the pump pulse was controlled by changing the path length of the pump pulse. The time origin and instrumental response function were determined by a cross correlation between the pump and probe pulses using a β-BaB_2O_4 crystal. All the measurements were performed at 294 K.

In Fig. 1(c), we show absorption (optical density: OD) spectra of Ca_2CuO_3 with the light electric field (E) ∥ and ⊥ b (the chain axis). We can see a peak structure at 2.1 eV polarized along b, which is attributable to the CT-gap transition. Circles in Fig. 1(c) show the excitation profile of photocurrent along b measured in a single crystal [38]. The photocurrent sharply increases from the absorption edge (∼1.75 eV) and saturates at around 1.9 eV below the CT-gap-transition peak. This result clearly demonstrates that the excitonic effect is negligibly small and that a resonant photoexcitation to the CT-gap transition produces unbound electron-hole pairs. This is attributable to the large transfer energy along the 1D chain relative to the intersite Coulomb repulsion [38].

Figure 2(a) shows photoinduced absorption (ΔOD) spectra by the 2.02-eV excitation measured with the time resolution of 200 fs. Excitation photon density x_{ph} is 0.077 photons (ph)/Cu [39]. In the CT-gap-transition region above 1.4 eV, ΔOD spectra show characteristic time dependence. At $t_d = 0.1$ ps, ΔOD is negative at around the absorption peak (1.8−2.4 eV), which is due to the bleaching of the CT band. For $t_d \geq 0.6$ ps, ΔOD has a positive peak at ∼1.8 eV. In Fig. 2(b), we replotted the ΔOD spectrum at 5 ps (open triangles), which is in good agreement with the spectral change [OD (314 K)-OD (294 K)] induced by an increase in temperature from 294 to 314 K (the broken line). This suggests that the positive ΔOD at ∼1.8 eV is due to the heating of the system. In Fig. 2(c), we show time characteristics of ΔOD at 1.82 and 2.20 eV. ΔOD at 1.82 eV becomes positive at $t_d \sim 0.25$ ps, indicating that the heating of the system occurs within ∼0.25 ps, while ΔOD at 2.20 eV is always negative reflecting both the bleaching and the heating-induced spectral change.

In the inner-gap region below 1.4 eV, ΔOD just after the photoexcitation ($t_d = 0.1$ ps) exhibits a broad structure centered at ∼0.5 eV, which almost decays at $t_d = 5.0$ ps. In Ca_2CuO_3, excitonic effects are negligible, so that this broad absorption is attributable to localized photocarriers. It is natural to consider that the localization is due to charge-phonon coupling, that is, a polaronic effect, since charge-spin coupling is small in 1D systems with large U [25,26]. The role of spin degree of freedom on the midgap absorption spectrum is discussed again later.

In Fig. 2(d), we show time profiles of ΔOD in the inner-gap region normalized at $t_d = 2$ ps. ΔOD has two components: a picosecond-decay component and an ultrafast (subpicosecond-decay) component; the former exists in four probe energies in common, while the latter decreases with increase of the probe energy and seems not to exist above 0.60 eV. The detailed analyses for the time profiles of ΔOD are reported in the Supplemental Material S4 [37].

To deduce spectral features of these two components, we show expanded ΔOD spectra for the weak excitation ($x_{ph} = 0.0077$ ph/Cu) and the strong excitation ($x_{ph} = 0.077$ ph/Cu) in Figs. 3(a) and 3(b), respectively, which are normalized at 0.60 eV. For the weak excitation, each ΔOD exhibits almost the same spectral shape, dominated mainly by the broad midgap absorption due to polarons. For $t_d < 0.3$ ps, a small deviation exists below 0.3 eV. For the strong excitation, the deviation is prominent below 0.4 eV, suggesting the presence of another component different from the midgap absorption, which shows an ultrafast decay.

In order to clarify this ultrafast-decay component below 0.4 eV, we extract its spectrum by subtracting from each ΔOD spectrum the component due to polarons, which is assumed to be the ΔOD spectrum at $t_d = 1.1$ ps. In Figs. 3(c)

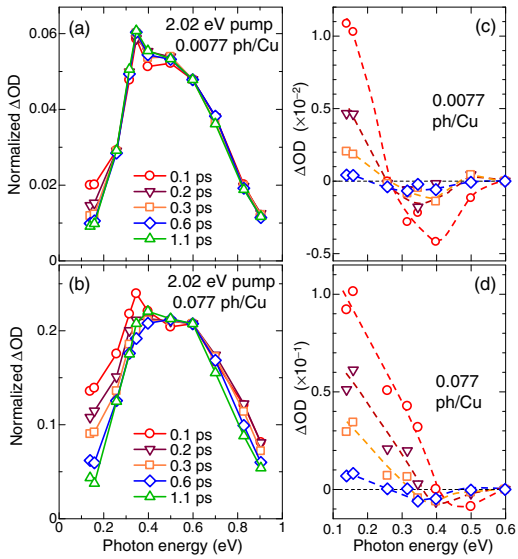

FIG. 3. (Color online) (a), (b) ΔOD spectra normalized at 0.60 eV for (a) weak excitation ($x_{ph} = 0.0077$ ph/Cu) and (b) strong excitation ($x_{ph} = 0.077$ ph/Cu). (c), (d) Spectra of ultrafast components $\Delta OD_{fast} = [\Delta\,OD - \alpha\Delta OD(1.1\,ps)]$ (see the text).

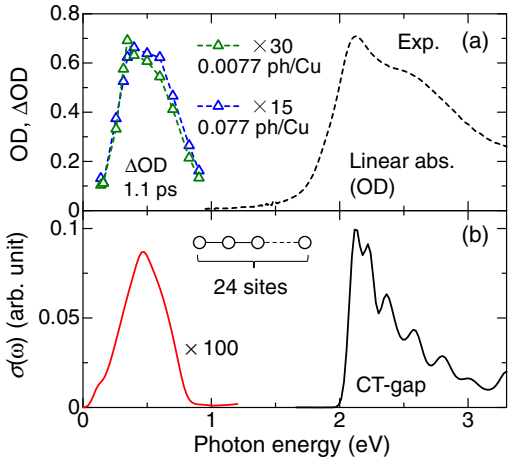

FIG. 4. (Color online) (a) OD spectrum and ΔOD spectra at 1.1 ps for weak excitation ($x_{ph} = 0.0077$ ph/Cu) and strong excitation ($x_{ph} = 0.077$ ph/Cu) in Ca_2CuO_3. (b) $\sigma(\omega)$ calculated for a 24-site chain of the extended Hubbard-Holstein model with a realistic parameters set for Ca_2CuO_3. Lower-energy and higher-energy parts correspond to phonon-assisted spin absorption and CT-gap absorption, respectively.

and 3(d), we show the ultrafast-decay component for the weak and strong excitations obtained by calculating $\Delta\,OD_{fast} = [\Delta\,OD - \alpha \times \Delta\,OD(t_d = 1.1\,ps)]$ at various delay times. α is adjusted so that ΔOD_{fast} is equal to zero at 0.60 eV. In both weak and strong excitations, ΔOD_{fast} increases monotonically with decreasing energy below 0.4 eV in common, showing photogenerations of metallic states. The energy position at which ΔOD crosses zero for $x_{ph} = 0.077$ ph/Cu is higher than that for $x_{ph} = 0.0077$ ph/Cu, consistent with the interpretation of ΔOD_{fast} by the Drude model. Such a Drude-like response originates from the nature of spin-charge separation.

To clarify the origin of the broad midgap absorption at around 0.5 eV, we calculate the real part of optical conductivity $\sigma(\omega)$ in an extended Hubbard-Holstein model at half filling, assuming that the observed midgap absorption appears as a consequence of a localized nature of electrons. The model contains nearest-neighbor transfer energy t, on-site Coulomb repulsion energy U, nearest-neighbor Coulomb repulsion energy V, Holstein-type electron-phonon coupling g, and Einstein phonon energy ω_0. In a previous publication by two of the present authors [40], $\sigma(\omega)$ for Sr_2CuO_3 has been calculated by using a realistic parameter set. Here, we determine a realistic parameter set for Ca_2CuO_3 by taking into account the difference of lattice constant and gap energy between Ca_2CuO_3 and Sr_2CuO_3. The estimated parameters are $t = 0.415$ eV, $U = 3.65$ eV, $V = 0.820$ eV, $g = 0.160$ eV, and $\omega_0 = 0.11$ eV. The $\sigma(\omega)$ is calculated for a 24-site chain by using the dynamical density-matrix renormalization group method, details of which have been given in Ref. [40].

We compare the observed OD and ΔOD with calculated $\sigma(\omega)$ in Fig. 4. The calculated Mott-gap (CT-gap) position is consistent with the observed one. Inside the gap, there is an absorption with a small spectral weight in the calculated $\sigma(\omega)$. The distribution of the weight is very similar to the observed ΔOD. The calculated midgap absorption is due to a phonon-assisted spin excitation [41]. Therefore, the broad ΔOD spectrum due to polarons is attributable to spin excitations coupled to phonons. This suggests that charge-spin coupling becomes effective via charge-phonon coupling.

As seen in Fig. 2(a), the midgap absorption due to polarons appears just after the photoirradiation ($t_d = 0.1$ ps). This suggests that most of photocarriers are relaxed to polarons within the time resolution of 200 fs and the higher time resolution is necessary to clarify their dynamical aspects. Figure 5(a) shows the time characteristic of ΔOD at 0.93 eV measured with the time resolution of 34 fs (open circles). Taking into account the probe-energy dependence

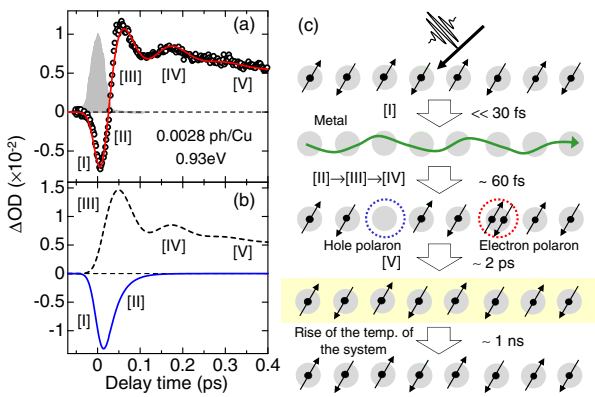

FIG. 5. (Color online) (a) Time profile of ΔOD at 0.93 eV (open circles) by the 2.02-eV pump ($x_{ph} = 0.0028$ ph/Cu). A cross-correlation profile of pump and probe pulses (gray shade) shows that the time resolution is 34 fs. The solid line is a fitting curve. (b) Components of the fitting curve in (a) (see text). (c) Schematic of photoinduced phenomena in Ca_2CuO_3. The green wavy line and the dashed circles represent the 1D photoinduced metallic state, and electron and hole polarons, respectively. The yellow shade represents the rise of the temperature of the system.

of ΔOD (see the Supplemental Material S3 [37]), we can attribute the initial decrease of OD to the formation of a metallic state and the subsequent increase of OD to the polaron formation. Negative ΔOD signals also exist in the extracted metallic responses shown in Figs. 3(c) and 3(d) [42]. On the positive ΔOD signal for $t_d > 0.02$ ps, an oscillation is observed.

To analyze the time characteristic of ΔOD, we adopted the following formula.

$$\begin{aligned}\Delta\mathrm{OD}(t_d) &= -\int_{-\infty}^{t_d} A_1 \exp\left(-\frac{t_d - t'}{\tau_1}\right) \exp\left(-\frac{t'^2}{\tau_0^2}\right) dt' \\ &+ \int_{-\infty}^{t_d} \left[1 - \exp\left(-\frac{t_d - t'}{\tau_4}\right) \cos\{\omega_1(t_d - t') + \theta_1\}\right] \\ &\times \left\{A_2 \exp\left(-\frac{t_d - t'}{\tau_2}\right) + A_3 \exp\left(-\frac{t_d - t'}{\tau_3}\right)\right\} \\ &\times \exp\left(-\frac{t'^2}{\tau_0^2}\right) dt'. \qquad (1)\end{aligned}$$

The first term represents the formation and decay of the metallic state, which is assumed to show an exponential decay. The second term represents the formation and decay of polarons accompanying a coherent oscillation expressed by the cosine-type damped oscillator, in which two exponential decays with time constants τ_2 and τ_3 are assumed and the relaxation time of the oscillation is expressed by τ_4. τ_0(=20 fs) is a parameter related to the time resolution, which was determined from the cross correlation of pump and probe pulses [the gray shade in Fig. 5(a)]. In Eq. (1), convolution integrals with the term $\exp(-t^2/\tau_0^2)$ corresponding to the time resolution (34 fs) are taken into account. The time profile of ΔOD can be well reproduced by Eq. (1) [the solid line in Fig. 5(a)]. The first and second terms were also shown in Fig. 5(b). Used parameter values are $\tau_1 = 26$ fs, $\tau_2 = 253$ fs, $\tau_3 = 7$ ps, $\tau_4 = 82$ fs, $\omega_1 = 255\ \mathrm{cm}^{-1}$, and $\theta_1 = -0.16\pi$. The success of the fit indicates that the metallic state is formed within the time resolution (34 fs) and decays with ∼30 fs, and polarons are formed within ∼60 fs. More detailed analysis of ΔOD of the midgap absorption revealed that the decay of polarons can be explained by bimolecular recombination processes, which is reported in the Supplemental Material S4 [37].

The initial phase θ_1 of the oscillation is small (-0.16π) and thus the oscillation is of the cosine type. This suggests that the oscillation is generated by a displacive excitation mechanism [43] and is attributed to the changes of equilibrium atomic positions associated with the polaron formation. A carrier on a Cu site will be stabilized by the displacements of neighboring four oxygen atoms, so that the corresponding oxygen breathing mode is a possible candidate of the coherent oscillation. Ca_2CuO_3 is a CT insulator, so that we have to take into account the asymmetry of electron and hole polarons, which was not discussed in this Rapid Communication. To fully understand the nature of polarons, further studies should be necessary.

From these analyses and discussions, the dynamical behaviors of the present photoinduced phenomena can be summarized as follows [Fig. 5(c)]: (I) First, a metallic state is photogenerated. Subsequently (II) it decays with the time constant of 30 fs and (III) the polaron formation occurs within 60 fs. (IV) It is accompanied by the coherent oscillation with the frequency of 255 cm^{-1}. (V) Finally, polaron recombination occurs.

Finally, we discuss the difference of photoresponses between Ca_2CuO_3 and the 2D cuprate, Nd_2CuO_4 [10,11]. In Fig. 2(c), we show the time characteristic of ΔOD at 1.30 eV of Nd_2CuO_4 measured with the time resolution of 200 fs, which reflects the heating effect similarly to ΔOD at 1.82 eV of Ca_2CuO_3 in the same figure. In Nd_2CuO_4, the rise time of ΔOD (∼0.2 ps) [11] is much shorter than that (∼0.45 ps) in Ca_2CuO_3. Such a difference can be explained by the different magnitudes of charge-phonon coupling between two compounds. In Ca_2CuO_3, photogenerated electrons and holes are localized as polarons more strongly than in Nd_2CuO_4. When photocarriers are strongly bound to the lattice, their recombination time is dominated by the encounter rate of electron and hole carriers. The larger charge-phonon coupling in 1D cuprates suppresses the carrier mobility and increases their recombination time compared to that in 2D cuprates. In contrast, in Nd_2CuO_4, the rise time of the heating effect (∼0.2 ps) corresponds to the carrier recombination time for the weak excitation case, which occurs probably through the emission of magnons [44–50]. These facts can explain the longer time constant for the heating or, equivalently, the slower decay time of carriers in Ca_2CuO_3 than in Nd_2CuO_4.

In summary, ultrafast charge and lattice dynamics due to photocarrier doping of the 1D cuprate, Ca_2CuO_3, was investigated by pump-probe absorption spectroscopy. We demonstrated that the photoirradiation of a femtosecond laser pulse generates a metallic state. Photocarriers are subsequently localized as polarons within ∼60 fs via charge-phonon coupling, producing a broad midgap absorption. Theoretical analyses with the extended Hubbard-Holstein model revealed that the spectral shape of the midgap absorption is dominated by a magnon sideband of the polaron absorption. This suggests that charge-spin coupling becomes effective via charge-phonon coupling in 1D Mott insulators.

This work was partly supported by a Grant-in-Aid for Scientific Research from the Japan Society for the Promotion of Science (Grants No. 25390061, No. 25247049, and No. 26287079). The theoretical part of this work is supported by MEXT HPCI Strategic Programs for Innovative Research (SPIRE) (hp130007, hp140215) and Computational Materials Science Initiative (CMSI). Numerical calculation was partly carried out at the K computer, the RIKEN Advanced Institute for Computational Science.

[1] M. Imada, A. Fujimori, and Y. Tokura, Rev. Mod. Phys. **70**, 1039 (1998).

[2] A. Cavalleri, Cs. Tóth, C. W. Siders, J. A. Squier, F. Ráksi, P. Forget, and J. C. Kieffer, Phys. Rev. Lett. **87**, 237401 (2001).

[3] C. Kübler, H. Ehrke, R. Huber, R. Lopez, A. Halabica, R. F. Haglund, Jr., and A. Leitenstorfer, Phys. Rev. Lett. **99**, 116401 (2007).
[4] V. R. Morrison, R. P. Chatelain, K. L. Tiwari, A. Hendaoui, A. Bruhács, M. Chaker, and B. J. Siwick, Science **346**, 445 (2014).
[5] P. Baum, D.-S. Yang, and A. H. Zewail, Science **318**, 788 (2007).
[6] M. Fiebig, K. Miyano, Y. Tomioka, and Y. Tokura, Science **280**, 1925 (1998).
[7] M. Rini, R. Tobey, N. Dean, J. Itatani, Y. Tomioka, Y. Tokura, R. W. Schoenlein, and A. Cavalleri, Nature (London) **449**, 72 (2007).
[8] M. Matsubara, Y. Okimoto, T. Ogasawara, Y. Tomioka, H. Okamoto, and Y. Tokura, Phys. Rev. Lett. **99**, 207401 (2007).
[9] D. Polli, M. Rini, S. Wall, R. W. Schoenlein, Y. Tomioka, Y. Tokura, G. Cerullo, and A. Cavalleri, Nat. Mater. **6**, 643 (2007).
[10] H. Okamoto, T. Miyagoe, K. Kobayashi, H. Uemura, H. Nishioka, H. Matsuzaki, A. Sawa, and Y. Tokura, Phys. Rev. B **82**, 060513(R) (2010).
[11] H. Okamoto *et al.*, Phys. Rev. B **83**, 125102 (2011).
[12] Y. Okimoto *et al.*, Phys. Rev. Lett. **103**, 027402 (2009).
[13] M. K. Liu *et al.*, Phys. Rev. Lett. **107**, 066403 (2011).
[14] P. Beaud *et al.*, Nat. Mater. **13**, 923 (2014).
[15] S. Iwai and H. Okamoto, J. Phys. Soc. Jpn. **75**, 011007 (2006).
[16] L. Perfetti *et al.*, Phys. Rev. Lett. **97**, 067402 (2006).
[17] Y. Kawakami, S. Iwai, T. Fukatsu, M. Miura, N. Yoneyama, T. Sasaki, and N. Kobayashi, Phys. Rev. Lett. **103**, 066403 (2009).
[18] M. Chollet *et al.*, Science **307**, 86 (2005).
[19] S. Iwai, M. Ono, A. Maeda, H. Matsuzaki, H. Kishida, H. Okamoto, and Y. Tokura, Phys. Rev. Lett. **91**, 057401 (2003).
[20] H. Matsuzaki *et al.*, Phys. Rev. Lett. **113**, 096403 (2014).
[21] H. Okamoto, H. Matsuzaki. T. Wakabayashi, Y. Takahashi, and T. Hasegawa, Phys. Rev. Lett. **98**, 037401 (2007).
[22] F. Schmitt, P. Kirchmann, U. Bovensiepen, R. G. Moore, L. Rettig, M. Krenz, J.-H. Chu, N. Ru, L. Perfetti, D. H. Lu, M. Wolf, I. R. Fisher, and Z.-X. Shen, Science **321**, 1649 (2008).
[23] M. Eichberger, H. Schäfer, M. Krumova, M. Beyer, J. Demsar, H. Berger, G. Moriena, G. Sciaini, and R. J. D. Miller, Nature (London) **468**, 799 (2010).
[24] L. Stojchevska, I. Vaskivskyi, T. Mertelj, P. Kusar, D. Svetin, S. Brazovskii, and D. Mihailovic, Science **344**, 177 (2014).
[25] M. Ogata and H. Shiba, Phys. Rev. B **41**, 2326 (1990).
[26] H. Eskes and A. M. Oleś, Phys. Rev. Lett. **73**, 1279 (1994).
[27] A. Lanzara *et al.*, Nature (London) **412**, 510 (2001).
[28] K. M. Shen, F. Ronning, D. H. Lu, W. S. Lee, N. J. C. Ingle, W. Meevasana, F. Baumberger, A. Damascelli, N. P. Armitage, L. L. Miller, Y. Kohsaka, M. Azuma, M. Takano, H. Takagi, and Z.-X. Shen, Phys. Rev. Lett. **93**, 267002 (2004).
[29] A. S. Mishchenko and N. Nagaosa, Phys. Rev. Lett. **93**, 036402 (2004).
[30] X. J. Zhou *et al.*, Phys. Rev. Lett. **95**, 117001 (2005).
[31] O. Rösch *et al.*, Phys. Rev. Lett. **95**, 227002 (2005).
[32] A. S. Mishchenko *et al.*, Phys. Rev. Lett. **100**, 166401 (2008).
[33] H. Matsueda, S. Sota, T. Tohyama, and S. Maekawa, J. Phys. Soc. Jpn. **81**, 013701 (2012).
[34] Chr. L. Teske and H. M.-Buschbaum, Z. Anorg. Allg. Chem. **379**, 234 (1971).
[35] S. Miyazawa and M. Mukaida, Appl. Phys. Lett. **64**, 2160 (1994).
[36] H. Kishida *et al.*, Phys. Rev. Lett. **87**, 177401 (2001).
[37] See Supplemental Material at http://link.aps.org/supplemental/10.1103/PhysRevB.91.081114 for the details about growths of thin films, pump-probe experiments, photoinduced change of absorption spectra for the 2.02-eV pump measured with the 34-fs time resolution, and analyses of time profile of ΔOD in the inner-gap region (<1 eV) measured with the 200-fs time resolution.
[38] M. Ono *et al.*, Phys. Rev. B **70**, 085101 (2004).
[39] $x_{\rm ph}$ was evaluated from $x_{\rm ph} = I_{\rm p}(1 - R_{\rm p})(1 - 1/e)/l_{\rm p}$, where $I_{\rm p}$, $l_{\rm p}$, and $R_{\rm p}$ are the excitation photon density per unit area, the absorption depth, and the reflection loss of the pump light, respectively.
[40] S. Sota and T. Tohyama, Phys. Rev. B **82**, 195130 (2010).
[41] H. Suzuura, H. Yasuhara, A. Furusaki, N. Nagaosa, and Y. Tokura, Phys. Rev. Lett. **76**, 2579 (1996).
[42] Higher-energy position at which ΔOD crosses zero for 34-fs time resolution measurement can be considered to be due to a high concentration of unbound electrons and holes at the initial stage of photoexcitation.
[43] H. J. Zeiger, J. Vidal, T. K. Cheng, E. P. Ippen, G. Dresselhaus, and M. S. Dresselhaus, Phys. Rev. B **45**, 768 (1992).
[44] K. Matsuda, I. Hirabayashi, K. Kawamoto, T. Nabatame, T. Tokizaki, and A. Nakamura, Phys. Rev. B **50**, 4097 (1994).
[45] A. Takahashi, H. Itoh, and M. Aihara, Phys. Rev. B **77**, 205105 (2008).
[46] Z. Lenarčič and P. Prelovšek, Phys. Rev. Lett. **111**, 016401 (2013).
[47] Z. Lenarčič and P. Prelovšek, Phys. Rev. B **90**, 235136 (2014).
[48] M. Eckstein and P. Werner, Phys. Rev. Lett. **110**, 126401 (2013).
[49] D. Golež, J. Bonča, M. Mierzejewski, and L. Vidmar, Phys. Rev. B **89**, 165118 (2014).
[50] E. Iyoda and S. Ishihara, Phys. Rev. B **89**, 125126 (2014).